Near-infrared characterization of gallium nitride photonic-crystal waveguides and cavities

U. Dharanipathy,* N. Vico Triviño, C. Yan, Z. Diao, J.-F. Carlin, N. Grandjean, and R. Houdré

Institut de Physique de la Matière Condensée, École Polytechnique Fédérale de Lausanne (EPFL), Station 3, Lausanne CH-1015, Switzerland

**Corresponding author: ulagalandha.dharanipathy@epfl.ch*

Received August 10, 2012; accepted September 24, 2012;
posted October 4, 2012 (Doc. ID 174126); published November 6, 2012

We report the design and optical characterization of fully suspended wire waveguides and photonic crystal (PhC) membranes fabricated on a gallium nitride layer grown on silicon substrate operating at 1.5 μm. W1-type PhC waveguides are coupled with suspended wires and are investigated using a standard end-fire setup. The experimental and theoretical dispersion properties of the propagating modes in the wires and photonic-crystal waveguides are shown. Modified L3 cavities with quality factors of up to 2200 and heterostructure cavities with quality factors of up to 5400 are experimentally demonstrated. © 2012 Optical Society of America

OCIS codes: 130.0130, 230.0230.

Gallium nitride (GaN) as a semiconductor technology has been used for high-power and high-temperature electronics and also as an emitter for ultraviolet (UV) and visible wavelengths due to its electronic and optical properties [1,2]. GaN-based photonic crystal (PhC) nanocavities are being increasingly studied for their emission properties for applications in lighting, displays, and integrated photonic biosensing [3–5]. However, a complete understanding of the propagation characteristics, mode dispersion, and photonic bandgap measurements of these PhC devices has been challenging, owing to technological difficulties in the processing of GaN. This platform is also interesting to explore high-Q cavities and nonlinear effects in the near-infrared (IR) region where two-photon absorption is not a limitation due to its wide bandgap. The added possibility of embedding active material in GaN would also enable various light–matter interaction studies along with the high-Q cavities.

In this Letter, fully suspended GaN wire waveguides of 3 μm width on a silicon substrate are reported. The wires in this case have to be suspended in air because of the larger refractive index of silicon (Si) compared to the GaN layer. These structures are mechanically held in place with the help of support tethers whose widths are set to 100 and 200 nm and intra-tether spacing set to 10 and 20 μm [6]. The widths of such tethers are found to be sufficient enough to hold the devices with mechanical stability ensuring that the wires do not collapse after the fabrication of the sample.

This GaN layer is grown along c-plane (0001) on top of an Si (111) substrate with an aluminum nitride (AlN) layer of 60 nm to allow for two-dimensional (2D) nucleation of GaN, and the cavities are aligned along [10–10]. The thickness of the GaN layer is set to 330 nm for single-mode operation within the PhC slabs. A thin layer (100 nm) of silicon dioxide (SiO_2) is deposited on GaN to act as a hard mask during the whole process. The structures are subsequently written by e-beam lithography. The SiO_2 is patterned with reactive ion etching (RIE), and the resist is removed. Afterwards, the etching of GaN by chlorine-based inductively coupled plasma is performed. The Si substrate is subsequently etched by RIE leading to a self-standing membrane including the wire waveguides, which are supported by tethers on either side as shown in Fig. 1. Finally, hydrofluorhydric acid solution is used to remove the hard mask. The details of the fabrication of the PhCs and the verticality of holes have also been reported elsewhere [5].

Standard photonic-crystal waveguides are fabricated by removing a single row of holes creating a line defect (W1 waveguide) for propagating light as shown in Fig. 1 (right bottom). The lattice constant (a) of the PhC is 600 nm, and the filling factor is 0.3. The nanowires are adiabatically tapered to match the width of the PhCW1 and enable a smooth transition into the coupling of the W1 mode from the nanowire section. The coupling of the slow-light mode in the W1 is optimized further by stretching the lattice constant in the beginning and end of the PhCW. The amount of lattice stretching is computed numerically after adjusting for the smaller refractive index of GaN using the method discussed and demonstrated in [7]. It is important to note that the PhC is fully membraned and is supported by the suspended waveguides making the entire structure freestanding from facet to facet, and hence, capable of avoiding polarization mixing and reducing propagation losses between TE and TM modes.

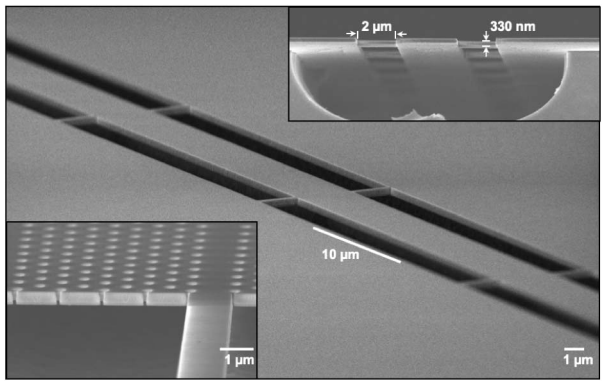

Fig. 1. Scanning electron microscope (SEM) image of GaN wire waveguides suspended with tethers. Top right: inset shows the cross section at the facet of the nanowire along with the undercut. Bottom left: inset shows the photonic-crystal W1 waveguide coupled by a tapered ridge waveguide.

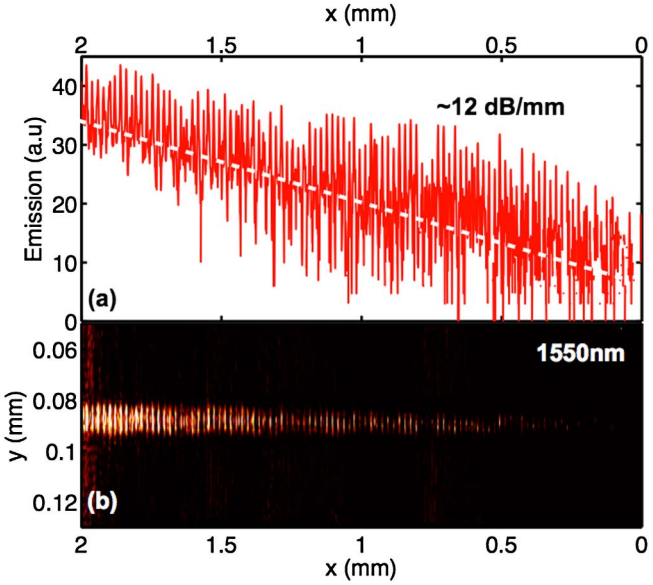

Fig. 2. (Color online) (a) Integrated intensity profile of the scattered light from the tethers along the propagation direction. (b) Real-space image of scattered light on top of the wire waveguide imaged with an infrared camera.

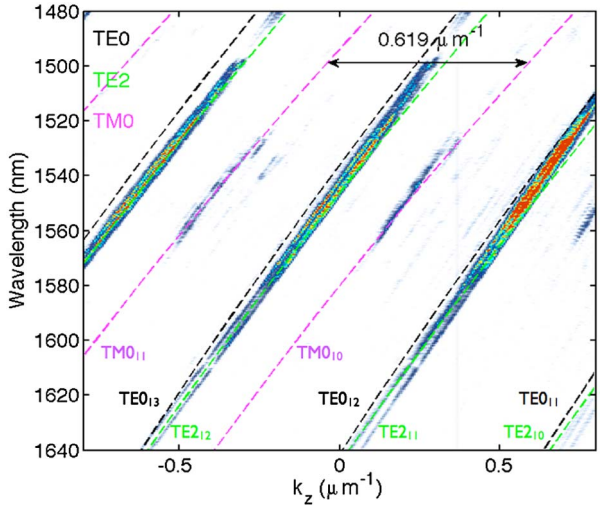

Fig. 3. (Color online) Experimental and numerical dispersion (dotted lines) of wire waveguides is shown. The folding period (G) corresponds to 0.619 μm^{-1} for all the modes. As each dispersion line is folded multiple times due to the tethers (grating), the folding order for each mode is indicated in the subscript of the mode labels.

The experimental setup used to measure the devices consists of a standard end-fire configuration with a tunable laser diode operating at 1.5 μm with polarization control. The nanowires suspended by the tethers are coupled using a tapered fiber at the input facet. In the first order, the tethers that are used to suspend the wire in this case can be assumed as uniform periodic scatterers that scatter the light in all directions, and this scattered light can be imaged using an infrared camera from the top of the sample as shown in Fig. 2(b). The decay of this scattered light can be used to estimate the losses in the nanowires as shown in Fig. 2(a). The propagation losses are estimated to vary from 10 to 12 dB/mm, which is a first reported loss number for GaN-based freestanding wire waveguides of this thickness.

The transmission through the nanowires can be further improved by optimizing the fabrication process for smoother sidewalls and a uniform bottom surface after etching the silicon underneath. The tethers placed on either side of the nanowire allow us to measure the dispersion of the propagating modes with Fourier imaging of this scattered light [8]. We performed 2D finite-element calculations for the theoretical mode dispersion with the dimensions used in our device. We obtain four TE modes and two TM modes for the GaN and AlN layers with material refractive indices 2.3 and 2.1, respectively.

The light emitted from the top of the sample is collected by an objective with numerical aperture of 0.45 to perform Fourier imaging. This field of view allows us to see several scatterers in real space and hence measure the dispersion of the propagating modes in the reciprocal space. The spacing of the tethers in the measured device is 10 μm, which gives rise to a folding period of 0.619 μm^{-1} in reciprocal space. The experimental and the superimposed theoretical results are shown in Fig. 3, and it can be clearly seen that the two strong lines representing the two TE modes are the even modes TE0 and TE2 and the weak line representing the TM mode is TM0. The mode numbering refers to lateral mode numbers as the membrane is single mode along the vertical direction. Given the symmetric nature of the waveguide, one would expect the TM mode to be not coupled in, but the faint coupling observed in Fig. 3. is attributed to the asymmetry created in our structure due to the thin layer of AlN under the GaN layer. All the modes appearing in the dispersion are the in-plane modes that are matched strongly with the mode profile coupled from the tapered fiber. The proximity of the TE dispersion lines, for instance between $TE0_{12}$ and $TE2_{11}$ observed in Fig. 3 where TEn_m denote the nth mode folded m times, is due to the fact that the folding orders are coincidentally close to one another when they are folded into the light cone due to the chosen grating spacing, which has also been confirmed with calculations.

The dispersion of PhC W1 is probed by using an objective with a high numerical aperture of 0.9, collecting the light that is scattered above the sample plane as shown in Fig. 4. The W1 mode can be clearly observed until the

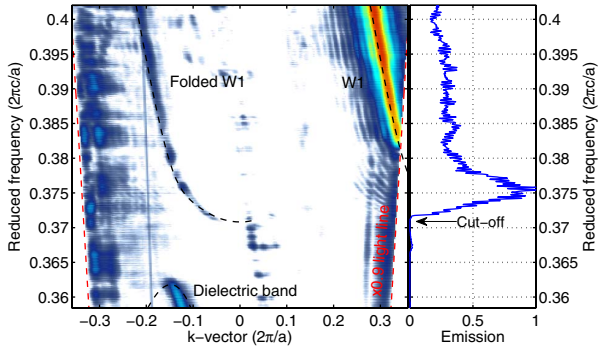

Fig. 4. (Color online) Dispersion of W1 even-mode propagation in the GaN PhC W1 waveguide with a grating. The dotted black line is the numerical computation performed with guided-mode expansion.

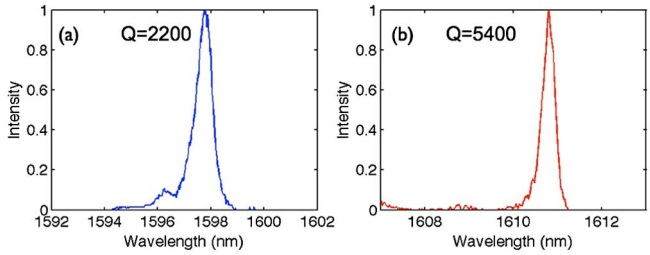

Fig. 5. (Color online) (a) Emission spectrum of a modified L3 cavity side coupled with eight rows from the W1.02 waveguide. (b) Emission spectrum of an inline heterostructure cavity with a barrier width of 10 a.

cut-off of the objective light line, below which the mode is truly guided and cannot be observed. The truly guided mode is probed with the help of a grating designed with a spacing of 2 a that folds the mode into the light cone and is imaged in the Fourier space. The emission of the output of the W1 waveguide allows us to ascertain the cut-off of the propagating mode and the onset of the photonic bandgap, which confirms with the measured dispersion curve very well. 2D guided-mode expansion [9] based calculations are performed to compute the numerical dispersion curve using refractive indices of 2.3 and 2.1 for GaN and AlN, respectively. They are superimposed on the experimental curve as shown in Fig. 4., and are in good agreement with each other.

Modified L3 cavities with the two holes next to the cavity shifted outward by 0.2 a [10] and heterostructure cavities [11] with a coupling barrier of 10 a are fabricated, and the experimentally measured quality factors (Q) are shown in Figs. 5(a) and 5(b). The numerical Q factors are computed with three-dimensional (3D) finite elements, and quality factors of 2900 and 50,000 (for the case of infinite barrier) are calculated for the two cavities respectively.

In summary, we have reported the fabrication of suspended nanowires and PhC membranes in GaN. We have also performed the first measurements of propagation losses and dispersion in GaN wires with losses on the order of 10 to 12 dB/mm, which are in the order of the reported loss figures for InP suspended nanowires [12]. This can be improved with further optimization of the fabrication process. We have also demonstrated a free-standing PhC W1 device coupled with a nanowire in the GaN platform that is highly polarization selective, and we have experimentally shown and theoretically verified the dispersion of the PhC waveguide mode with the use of Fourier imaging. High-Q cavity designs have been studied and a heterostructure cavity with a Q factor of up to 5400 has been achieved, which could be used in the investigation of light–matter interaction studies involving active material in the GaN membrane.

The authors acknowledge support from the Swiss National Center of Competence in Research—Quantum Photonics.

References

1. S. N. Mohammad, A. A. Salvador, and H. Morkoç, Proc. IEEE **83**, 1306 (1995).
2. H. Matsubara, S. Yoshimoto, H. Saito, Y. Jianglin, Y. Tanaka, and S. Noda, Science **319**, 445 (2008).
3. A. David, T. Fujii, R. Sharma, K. McGroddy, S. Nakamura, S. P. DenBaars, E. L. Hu, C. Weisbuch, and H. Benisty, Appl. Phys. Lett. **88**, 061124 (2006).
4. C. Meier, K. Hennessy, E. D. Haberer, R. Sharma, Y.-S. Choi, K. McGroddy, S. Keller, S. P. DenBaars, S. Nakamura, and E. L. Hu, Appl. Phys. Lett. **88**, 031111 (2006).
5. N. Vico Triviño, G. Rossbach, U. Dharanipathy, J. Levrat, A. Castiglia, J.-F. Carlin, K. A. Atlasov, R. Butté, R. Houdré, and N. Grandjean, Appl. Phys. Lett. **100**, 071103 (2012).
6. A. Talneau, K. H. Lee, S. Guilet, and I. Sagnes, Appl. Phys. Lett. **92**, 061105 (2008).
7. J. P. Hugonin, P. Lalanne, T. P. White, and T. F. Krauss, Opt. Lett. **32**, 2638 (2007).
8. N. Le Thomas, R. Houdré, M. V. Kotlyar, D. OBrien, and T. F. Krauss, J. Opt. Soc. Am. B **24**, 2964 (2007).
9. L. C. Andreani and D. Gerace, Phys. Rev. B **73**, 235114 (2006).
10. Y. Akahane, T. Asano, B. Song, and S. Noda, Nature **425**, 944 (2003).
11. B. Song, S. Noda, T. Asano, and Y. Akahane, Nat. Materials **4**, 207 (2005).
12. A. Talneau, K. H. Lee, and I. Sagnes, IEEE Photon. Technol. Lett. **21**, 775 (2009).